UDC 547.1-304.2:546.224

R.E. Khoma [a], V.N. Baumer [b], V.O. Gelmboldt [c], N.F. Fedko [a], V.V. Menchuk [a], S.V. Vodzinsky [a], Yu.V. Ishkov [a], I.M. Rakipov [d], D.V. Menchuk [a]

SPECTRAL CHARACTERISTICS OF INTERACTION PRODUCTS IN $SO_2-CH_3CH(OH)CH_2NH_2-H_2O$ AND $SO_2-CH_3CH(OH)CH_2NH_2-CH_2O-H_2O$ SYSTEMS

[a] Odesa I.I. Mechnikov National University, Odesa, Ukraine
[b] Institute for Single Crystals, National Academy of Sciences of Ukraine, Kharkiv, Ukraine
[c] Odesa National Medical University, Odesa, Ukraine
[d] A.V. Bogatsky Physico-Chemical Institute, National Academy of Sciences of Ukraine, Odesa, Ukraine

Interaction in the systems «sulfur(IV) oxide–2-hydroxypropylamine (MiPA)–water» and «sulfur(IV) oxide–MiPA–paraform–water» leads to the formation of 2-hydroxypropylammonium sulfite $[CH_3CH(OH)CH_2NH_3]_2SO_3$ (I) and N-(2-hydroxypropyl)aminomethanesulfonic acid $CH_3CH(OH)CH_2N^+H_2CH_2SO_3^-$ (II), respectively. These compounds, upon independent recrystallization from aqueous solution, are transformed into 2-hydroxypropylammonium sulfate $[CH_3CH(OH)CH_2NH_3]_2SO_4$ (III) as a result of hydrolytic transformations. The obtained products were characterized by the methods of elemental and X-ray structural analysis, IR, Raman, ^1H and ^{13}C NMR spectroscopy, and mass spectrometry. Compound III crystallizes in triclinic class (space group P-1, a=9.0753(8) Å, b=10.3038(7) Å, c=13.6845(14) Å, α=99.491(7)^0, β=94.712(8)^0, γ=90.119(7)^0, V=1257.7(2)Å^3, Z=4). The IR spectrum of salt I shows the valence vibrations of ν(SO) sulfite anion (ν_1 and ν_3), represented by bands at 912 and 954 cm^{-1}, respectively. The vibration δ_s (ν_2) of SO_3^{2-} ion is observed in the IR spectrum as relatively intense bands at 610 and 621 cm^{-1}. In the IR spectrum of compound II, the vibrations $\nu_{as}(SO_2)$ appear as a doublet at 1234 and 1208 cm^{-1}; $\nu_s(SO_2)$ is represented by a multiplet of lines in the 1180–1030 cm^{-1} region. Upon attempted recrystallization from aqueous solution, the ammonium sulfite salt MiPA (I) undergoes hydrolytic sulfoxidation, converting into the corresponding sulfate III. Similarly, the N-alkylated AMSA derivative II is oxidized via a hydrolytic redox process to sulfate III as well.

Keywords: sulfur dioxide, 2-hydroxypropylamine, ammonium sulfite, ammonium sulfate, condensation, sulfoxidation, spectral characteristics.

DOI: 10.32434/0321-4095-2025-163-6-113-121

Introduction

Ethanolamines are precursors of protic ionic liquids [1], enabling the development of low-toxic, bioavailable compounds aligned with green chemistry principles. They are widely used in chemisorption processes to capture acidic gases (CO_2, SO_2, etc.) [2–4], and serve as potential vitrifying agents for long-term cryopreservation of biological tissues and organs [5].

Elucidation of the structure and physicochemical

properties of the interaction products in the systems $SO_2-RNH_2-H_2O$, $SO_2-RNH_2-H_2O-O_2$, and $SO_2-RNH_2-CH_2O-H_2O$ provides a foundation for developing theoretical principles for the a priori selection of sulfur(IV) dioxide chemisorbents and the search for new biologically active N,S-containing compounds [4,6].

In this study, 2-hydroxypropylamine (MiPA) was selected as a model ethanolamine. The synthesis and identification of the interaction products in the systems «sulfur(IV) dioxide–MiPA–water» and «sulfur(IV) dioxide–MiPA–formaldehyde–water» are described. These include the novel compounds 2-hydroxypropylammonium sulfite (I) and N-(2-hydroxypropyl)aminomethanesulfonic acid (II), respectively, as well as the product of their independent recrystallization from aqueous solution – 2-hydroxypropylammonium sulfate (III).

Experimental

N-(2-hydroxypropyl)ammonium sulfite (I)

A solution of MiPA (0.02 mol) in 30 ml of water was poured into a thermostated cell (20^{0}C) and SO_2 was bubbled through it at a rate of 50 ml/min^{-1} for 45 min (pH≤1.0; t=20^{0}C). The resulting solution was kept at room temperature in air until water was completely removed. The isolated white crystalline product **I** (2.30 g, yield 99.01%) was used without further purification.

Found, %: C 31.25; H 8.84; N 12.19; S 14.21. $C_6H_{20}N_2O_5S$. Calculated, %: C 31.02; H 8.68; N 12.06; S 13.80. M 232.30.

MS EI **I**: $[M_{MiPA}]^+$ (m/z 75, I, 13%); $[SO_2]^+$ (m/z 64, I, 100%); $[SO]^+$ (m/z 48, I, 67%); $[C_2H_5O]^+$ (m/z 45, I, 41%); $[M_{MiPA}-CH_2OH]^+$ (m/z 44, I, 12%); $[M_{MiPA}-CH_2OH-H]^+$ (m/z 43, I, 49%); m/z 42, I, 38%; $[M_{MiPA}-NH_3-H_2O]^+$ (m/z 40, I, 19%); $[S]^+$ (m/z 32, I, 82%).

IR **I** [ν, cm^{-1}]: 3370–3322 br.w., 3220–3207 br.m., 3036 br.m. [ν(OH), $\nu_{as,s}(^+NH_3)$]; 2985 s., 2962 s., 2927 s., 2870 s., 2823–2811 br.s. [ν(CH_3), ν(CH_2), ν(CH)]; 1615 m. [$\delta_{as}(^+NH_3)$]; 1521 s. [$\delta_s(^+NH_3)$]; 1454 sh., 1403 w. [δ(CH_2), δ(CH_3)]; 1206 sh., 1189 sh. [g($^+NH_3$)]; 1153 w., 1120 sh. [ν(CO), γ(CH_3)]; 1090 s., 1058 s., 1023 s. [δ(COH), ν(CN), γ(CH_3), γ($^+NH_3$), ν(CC)$_{as}$]; 1007 s. [γ(CH_3), g($^+NH_3$)]; 954 w. [γ(CH_2), $\nu_3(SO_3^{2-})$]; 912 s. [ω($^+NH_3$), $\nu_1(SO_3^{2-})$]; 876 s., 836 s. [γ(CH_3), ω($^+NH_3$), γ(CH_2)]; 680 s. [δ(CCO)$_s$]; 665 s., 621 w. [δ(CCO)$_s$, $\nu_2(SO_3^{2-})$]; 564 s., 519 m. [δ(CCO)$_{as}$]; 505 sh. [τ(HOCC), $\nu_4(SO_3^{2-})$]; 478 s., 435 s. [δ(CCO)$_s$, $\nu_4(SO_3^{2-})$]; 413 w. [δ(CCO)$_{as,s}$].

Raman spectrum **I** [ν, cm^{-1}]: 3349 w, 3322 w, 3315 w., 3311 w., 3304 w., 3281 w., 3270 w., 3251 w., 3237 w., 3227 w., 3224 w., 3210 w., 3006 s. [ν(OH), $\nu_{as,s}(^+NH_3)$]; 2991 s., 2968 s., 2935 s., 2916 s., 2877 m. [ν(CH_3), ν(CH_2), ν(CH)]; 1616 w. [$\delta_{as}(^+NH_3)$]; 1515 w. [$\delta_s(^+NH_3)$]; 1452 w., 1408 w. [δ(CH_2), δ(CH_3)]; 1213 w. [δ($^+NH_3$)]; 1157 w., 1127 m., 1116 m. [ν(CO), γ(CH_3)]; 1096 m., 1067 w., 1036 s. [δ(COH), ν(CN), γCH_3)]; 1004 s. [γ(CH_3), γ($^+NH_3$)]; 962 w. [γ(CH_2), $\nu_3(SO_3^{2-})$]; 922 m., 882 w. [ω($^+NH_3$), $\nu_1(SO_3^{2-})$]; 846 m., 826 m. [γ(CH_3), ω($^+NH_3$), γ(CH_2)]; 653 w., 631 w., 624 w. [δ(CCO)$_s$, $\nu_2(SO_3^{2-})$]; 691 m. [δ(CCO)$_s$]; 570 m., 525 m. [δ(CCO)$_{as}$]; 487 m., 441 m. [δ(CCO)$_s$, $\nu_4(SO_3^{2-})$].

N-(2-hydroxypropyl)aminomethanesulfonic acid (II)

Paraformaldehyde was added to 25 ml of an aqueous solution containing 0.01 mol of MiPA in an equimolar ratio while cooling (t≤10^{0}C) and left for 24 h; SO_2 was bubbled through the resulting solution to pH≤1.0, followed by keeping the reaction mixture at room temperature until the water evaporated completely. White crystalline product **II** (1.65 g, yield 97.52%) was isolated, which was used without further purification. The structure of the obtained product was confirmed by various physicochemical methods.

Found, %: C 28.12; H 6.33; N 8.45; S 18.64. $C_4H_{11}NO_4S$. Calculated, %: C 28.40; H 6.55; N 8.28; S 18.95. *M* 169.20.

MS EI: **II**: $[SO_2]^+$ (*m/z* 64, *I*, 100%); $[M-SO_3-CH_2-NH_3]^+$ (*m/z* 58, *I*, 13%); $[M-SO_3-CH_2-NH_3-H]^+$ (*m/z* 57, *I*, 19%); $[SO]^+$ (*m/z* 48, *I*, 48%); $[C_2H_5O]^+$ (*m/z* 45, *I*, 16%); $[M_{MiPA}-CH_2OH]^+$ (*m/z* 44, *I*, 31%); $[M_{MiPA}-CH_2OH-H]^+$ (*m/z* 43, *I*, 91%); *m/z* 42, *I*, 46%; $[M-SO_3-NH_3-CH_2OH]^+$ (*m/z* 41, *I*, 21%);

MS FAB **II**: $[M]^+$ (*m/z* 169, *I*, 9%); $[M-H]^+$ (*m/z* 168, *I*, 11%); $[M-NH_3]^+$ (*m/z* 152, *I*, 10%); $[M-H_2O-2H]^+$ (*m/z* 149, *I*, 12%); $[M-CH_2OH+H]^+$ (*m/z* 139, *I*, 8%); $[M-CH_2OH]^+$ (*m/z* 138, *I*, 26%); $[M-CH_2OH-H]^+$ (*m/z* 137, *I*, 50%); $[M-CH_2OH-2H]^+$ (*m/z* 136, *I*, 50%); $[M-SO-H]^+$ (*m/z* 120, *I*, 9%); $[M-SO_2+H]^+$ (*m/z* 106, *I*, 22%); $[M-SO_2]^+$ (*m/z* 105, *I*, 7%); $[M-SO_2-H]^+$ (*m/z* 104, *I*, 17%); $[M-MiPA]^+$ (*m/z* 94, *I*, 9%); $[M-SO_3+H]^+$ (*m/z* 90, *I*, 19%); $[M-SO_3]^+$ (*m/z* 89, *I*, 19%); $[M-SO_3-H]^+$ (*m/z* 88, *I*, 32%); $[SO_3]^+$ (*m/z* 80, *I*, 13%); $[M_{MiPA}+2H]^+$ (*m/z* 77, *I*, 15%); $[M_{MiPA}+H]^+$ (*m/z* 76, *I*, 32%); *m/z* 69, *I*, 11%; *m/z* 68, *I*, 10%; $[SO_2]^+$ (*m/z* 64, *I*, 9%); *m/z* 63, *I*, 13%; $[M-SO_3-CH_2-NH_3-H]^+$ (*m/z* 57, *I*, 9%); $[M-SO_3-NH_3-CH_2OH]^+$ (*m/z* 41, *I*, 16%); $[M-SO_3-NH_3-CH_2OH-H]^+$ (*m/z* 40, *I*, 14%); $[M-SO_3-NH_3-CH_2OH-2H]^+$ (*m/z* 39, *I*, 20%).

IR **II** [ν, cm^{-1}]: 3413 s., 3168 sh., 3076 s., 3026 s. [ν(OH), $\nu_{as,s}(^{+}NH_2)$]; 2994 s., 2975 s., 2936 sh., 2889 s., 2836 s. [ν(CH_3), ν(CH_2), ν(CH)]; 1625 sh., 1583 s. $\delta_{as,s}(^{+}NH_2)$; 1463 m., 1457 m., 1448 m., 1431 w. [δ(CH_2), δ(CH_3)]; 1271 s. [δ(COH)]; 1234 s. [δ(COH), $\nu_{as}(SO_2)$]; 1208 s. [$g(^{+}NH_2)$, $\nu_{as}(SO_2)$]; 1180 s., 1136 s., 1116 m. [$\gamma(^{+}NH_2)$, ν(CO), γ(CH_3)]; 1091 s. [ν(CN), δ(COH), $\nu_s(SO_2)$]; 1063 s. [γ(CH_3), $\gamma(^{+}NH_2)$, $\nu_s(SO_2)$]; 1050 w., 1030 s. [$\nu(CC)_{as}$, γ(CH_3), ν(CN), $_s(SO_2)$]; 937 w. [γ(CH_2), ω(NH_2)]; 917 m. [γ(CH_3), $\omega(^{+}NH_2)$]; 805 m. [γ(CH_2)]; 778 m. $[\nu(CC)_s]$; 624 m. $[\delta(CCO)_s]$; 551 s., 547 s. [ν(S−O)]; 529 w., 517 sh. $[\delta(CCO)_{as}]$; 482 m., 457 sh., 442 w. [τ(HOCC), $\delta(CCO)_s$], 413 w. $[\delta(CCO)_{as}]$.

*N-(2-hydroxypropyl)ammonium sulfate **(III)***

When attempting to recrystallize compound I (2.30 g) from an aqueous solution (30 ml), a white crystalline product **III** was isolated (2.44 g, yield 99.25%).

Found, %: C 28.91; H 8.21; N 11.15; S 13.14. $C_6H_{20}N_2O_6S$. Calculated, %: C 29.02; H 8.12; N 11.28; S 12.91. *M* 248.29.

MS EI **III**: $[M_{MiPA}]^+$ (m/z 75, I, 8%); $[SO_2]^+$ (m/z 64, I, 87%); $[SO]^+$ (m/z 48, I, 80%); $[C_2H_5O]^+$ (m/z 45, I, 29%); $[M_{MiPA}-CH_2OH]^+$ (m/z 44, I, 17%); $[M_{MiPA}-CH_2OH-H]^+$ (m/z 43, I, 34%); m/z 42, I, 30%; $[M_{MiPA}-NH_3-H_2O+H]^+$ (m/z 41, I, 10%); $[S]^+$ (m/z 32, I, 100%).

IR **III** [ν, cm^{-1}]: 3375−3309 sh., 3219 sh., 3045 w., 3033 br.m. $[\nu(OH), \nu_{as,s}(^{+}NH_3)]$; 2985 sh., 2963 w., 2928 s., 2870 sh. [ν(CH_3), ν(CH_2), ν(CH)]; 1615 m. $[\delta_{as}(^{+}NH_3)]$; 1522 m. $[\delta_s(^{+}NH_3)]$; 1458 w., 1446 w., 1441 w., 1403 w. [δ(CH_2), δ(CH_3)]; 1235 sh. $[g(^{+}NH_3)]$; 1153 sh. [ν(CO)]; 1120 sh. [γ(CH_3), $\nu_3(SO_4^{2-})$]; 1087 s., 1056 s., 1022 s. [δ(COH), ν(CN), γ(CH_3), $\gamma(^{+}NH_3)$, $\nu(CC)_{as}$]; 1006 s. [γ(CH_3)]; 986 m. [$\gamma(^{+}NH_3)$, $\nu_1(SO_4^{2-})$]; 956 w. [γ(CH_2)]; 914 s. $[\omega(^{+}NH_3)]$; 877 s., 837 s. [γ(CH_3), $\omega(^{+}NH_3)$, γ(CH_2)]; 681 s., 610 w. $[\nu_4(SO_4^{2-}), \delta(CCO)_s]$; 564 s., 519 m. $[\delta(CCO)_{as}]$; 505 sh. [τ(HOCC)]; 478 s. $[\delta(CCO)_s]$; 436 sh., 433 m. $[\nu_2(SO_4^{2-})]$; 416 w., 409 w. $[\delta(CCO)_{as,s}]$.

Raman spectrum **III** [ν, cm^{-1}]: 3344 w., 3315 w., 3310 w., 3303 w., 3279 w., 3269 w., 3246 w., 3238 w., 3201 w., 3001 m. $[\nu(OH), \nu_{as,s}(^{+}NH_3)]$; 2985 m., 2965 s., 2931 s., 2905 s. [ν(CH_3), ν(CH_2), ν(CH)]; 1616 w. $[\delta_{as}(^{+}NH_3)]$; 1508 w. $[\delta_s(^{+}NH_3)]$; 1446 w. [δ(CH_2), δ(CH_3)]; 1205 w., 1192 w. $[\gamma(^{+}NH_3)]$; 1150 w. [ν(CO)]; 1111 m. [γ(CH_3), $\nu_3(SO_4^{2-})$]; 1087 m., 1027 s., 997 m. [δ(COH), ν(CN), γ(CH_3), $\gamma(^{+}NH_3)$, $\nu(CC)_{as}$]; 971 s. [$g(CH_2)$, $\nu_1(SO_4^{2-})$]; 916 m. $[\omega(^{+}NH_3)]$; 874 w., 839 w., 818 m. [γ(CH_3), $\omega(^{+}NH_3)$, γ(CH_2)]; 682 m., 648 w., 623 w. $[\nu_4(SO_4^{2-}), \delta(CCO)_s]$; 560 m., 514 m. $[\delta(CCO)_{as}]$; 477 m., 434 m. $[\delta(CCO)_s, \nu_2(SO_4^{2-})]$.

Elemental analysis of carbon, hydrogen, and nitrogen was performed using a CHN elemental analyzer, while sulfur content was determined using the Schöniger method, as described in [7]. IR absorption spectra were recorded on a Spectrum BX II FT-IR System spectrophotometer (Perkin-Elmer) in the 4000−350 cm^{-1} range, with samples prepared as KBr pellets. Raman spectra were obtained using a DXR Raman Microscope (Thermo Scientific). Electron impact (EI) mass spectra were recorded on an MX-1321 instrument using direct sample insertion into the ion source with an ionizing electron energy of 70 eV.

Single-crystal X-ray diffraction study of compound **III** was performed on an Xcalibur-3 diffractometer (Oxford Diffraction Ltd.) equipped with a Sapphire-3 CCD detector. Structure was solved using the SHELXT program [8]. The structure was refined by the full-matrix least-squares method on F^2 in the anisotropic approximation with the SHELXL program [9]; hydrogen atoms were refined in the isotropic approximation using a riding model. The WinGX and ORTEP programs [10] were used for structural analysis and preparation of illustrations. The main crystallographic data and final refinement parameters are summarized in Table 1. Selected geometric parameters of compound III are listed in Tables 2 and 3. The complete crystallographic data for compound III have been deposited with the Cambridge Crystallographic Data Centre (CCDC 2466061).

The center of gravity of intermolecular hydrogen bonds was calculated using the formula $\nu_{gc}(OH) = \frac{\sum A_i \cdot \nu_i}{\sum A_i}$ (where A_i and ν_i are the absorption and frequency, respectively) in the region of 4000−3500 cm^{-1} [11].

Results and discussion

Mass spectra of salts **I** and **III**, as well as compound **II**, exhibit an intense peak at $[MMiPA-CH_2OH]^+$ characteristic of ethanolamine fragmentation products [12]. The fragmentation patterns of MiPA observed in the mass spectra of salts **I** and **III** are in good agreement with the tabulated mass spectrum of MiPA[1].

The X-ray single-crystal analysis of compound **III** reveals that the structure contains four $(C_3H_{10}NO)^+$ cations and two sulfate SO_4^{2-} anions in the asymmetric

[1] 2-Propanol, 1-amino- https://webbook.nist.gov/cgi/cbook.cgi?ID=C78966&Mask=268.

unit of the cell (Fig. 1), with all amino nitrogen atoms being protonated. Bond lengths and valence angles (Tables 2 and 3) show no significant anomalies. The O–H···O and N–H···O hydrogen bonds form in the structure between the cations and the oxygen atoms of the sulfate anions (Table 4). Analysis of the crystal packing of compound **III** (Fig. 2) indicates that this hydrogen-bonding system forms two-dimensional networks lying in the (001) crystallographic planes. Notably, this structural feature affects the crystal habit of compound **III**, which occurs as thin plate-like crystals.

Rietveld analysis of the powder X-ray diffraction pattern of compound **III** (Fig. 3) indicates that the compound is pure, single-phase, and its structure is fully consistent with that determined by single-crystal X-ray diffraction. The diffraction pattern shows a pronounced preferred orientation effect of the crystallites (planes (001)), which is in good agreement with the plate-like crystal habit of the compound.

Assignment of vibrational modes of [MiPAH]z cations in the IR and Raman spectra of salts **I** and **III**, as well as the $CH_3CH(OH)CH_2H_2$-fragment in the IR spectrum of compound **II**, was performed

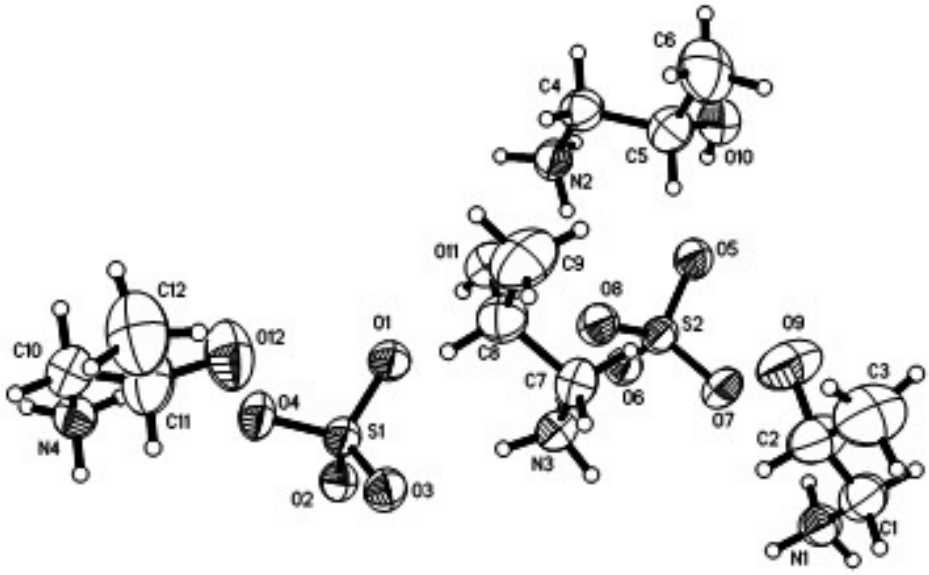

Fig. 1. Atom numbering scheme and thermal ellipsoids (probability level 50%) for the structure **III**

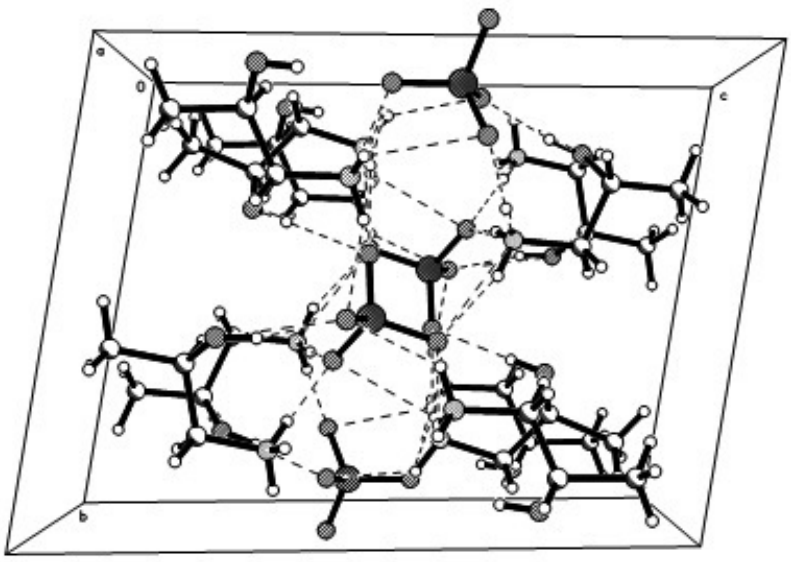

Fig. 2. Projection *0yz* of the structure **III**. Hydrogen bonds are represented by dashed lines

using literature data [11,13]. The IR and Raman spectra of compounds **I**–**III** display broad bands in the 3413–3001 cm^{-1} region, attributed to symmetric and asymmetric stretching vibrations $\nu(NH_3)$, $\nu(NH_2)$, and $\nu(OH)$. A multiplet with a maximum above 3500 cm^{-1} corresponds to $\nu(OH)$ vibrations in aggregated particles containing intermolecular hydrogen bonds of the OH···N type. The relative strength of intermolecular hydrogen bonds in the synthesized compounds, estimated by the center-of-gravity frequencies [11], decreases in the order MiPA>**III**>**I**>**II** (ν_{gc}(OH), cm^{-1}: 3525 for MiPA [11]; 3634 for **III**; 3704 for **I**; and 3741 for **II**), indicating that salt formation weakens these interactions.

Table 1

Crystallographic data, X-ray diffraction conditions, and structure refinement parameters for compound III

Characteristic	Value
Formula	$C_6H_{20}N_2O_6S$
M_r	248.30
T, K	293(2)
Crystal system	triclinic
space group	P-1
Unit-cell parameters:	9.0753(8)
a, Å	
b, Å	10.3038(7)
c, Å	13.6845(14)
α, °	99.491(7)
β, °	94.712(8)
γ, °	90.119(7)
V, Å^3	1257.7(2)
Z	4
ρ, g/cm^3	1.311
Absorption coefficient μ(MoK$_\alpha$), mm^{-1}	0.270
Range θ, °	2.991–25.999
Index ranges	–11≤h≤9; –11≤k≤12; –16≤l≤16
Crystal size, mm	0.340×0.220×0.070
F_{000}	536
Transmission coefficient T_{min}/T_{max}	0.914/0.981
Reflections collected	4861
Independent reflections with $I_{hkl}>2\sigma(I)$	2440
R_{int}	0.0944
Completeness, %	98.5
Refinement method	Full-matrix least-squares on F^2
Number of parameters refined	282
R_F/wR^2 for observed reflections	0.0787/0.1802
R_F/wR^2 for all independent reflections	0.1305/0.2182
S	0.979
$\Delta\rho_{min}/\Delta\rho_{max}$, e/Å^3	–0.288/0.295

In the IR spectrum of compound **II**, the asymmetric and symmetric stretching vibrations of cations $\nu_{as,s}(^{+}NH_2)$ are observed at 3413 cm^{-1} and in the 3168–3026 cm^{-1} range, respectively. Bending vibrations $\delta_{as,s}(^{+}NH_2)$ appear at 1625–1500 cm^{-1}. The asymmetric and symmetric stretching vibrations of ammonium cations $\nu_{as,s}(^{+}NH_3)$ in the IR spectra of salts **I** and **III** are observed as broad, intense bands around 3036 cm^{-1}; in the Raman spectra, they appear as medium-intensity singlets at 3006 and 3001 cm^{-1}, respectively.

The fact of proton transfer with the formation of ammonium groups in salts **I** and **III** is confirmed by the IR bands of medium intensity for asymmetric NH bending at 1615 cm^{-1} and strong symmetric scissoring vibrations at 1520 cm^{-1}. In the Raman spectra, they appear as weak singlets at 1624, 1616, 1515, and 1508 cm^{-1}, respectively.

In the IR spectrum of compound **II**, $d(NH_2)$ vibrations appear in the 1625–1507 cm^{-1} range as a shoulder at 1583 cm^{-1} and two bands of strong (1583 cm^{-1}) and weak (1507 cm^{-1}) intensity. Bands in the regions 1210–1180, ~1060, and ~1005 cm^{-1} are attributed to librational modes, while those in the 937–818 cm^{-1} range correspond to wagging vibrations of $^{+}NH_3$ and $^{+}NH_2$ groups.

The free pyramidal sulfite ion SO_3^{2-} belongs to the C_{3v} point group and exhibits four fundamental vibrational modes: ν_1 (A_1) – 967 cm^{-1}, ν_2 (A_1) – 620 cm^{-1}, ν_3 (E) – 933 cm^{-1}, and ν_4 (E) – 469 cm^{-1}. Due to the low local symmetry of the ion in the crystal, all fundamental vibrations are expected to be IR- and Raman-active, and the degeneracy of the E modes is fully lifted [6].

In the IR spectrum of salt I, the S–O stretching vibrations ν_1 and ν_3 of SO_3^{2-} ion are observed as strong and weak bands at 912 and 954 cm^{-1}, respectively. In the Raman spectrum, these appear as three lines at 962, 922, and 882 cm^{-1}. Splitting of the ν_3 (E) Raman band into two components suggests a distortion of the sulfite ion geometry in the crystal lattice of **I**, as well as the involvement of the ion in inequivalent hydrogen bonds of the OH···O and NH···O types (similar to [6]). Additionally, a distinct shoulder at 505 cm^{-1} and two strong bands at 478 and 435 cm^{-1} in the IR spectrum, along with two Raman lines at 487 and 441 cm^{-1}, are attributed to the splitting of the doubly degenerate out-of-plane deformation mode ν_4(E) of ion. The symmetric bending vibration δ_s (ν_2) of SO_3^{2-}

ion is observed in the IR spectrum as relatively intense bands at 610 and 621 cm^{-1}, and in the Raman spectrum as weak lines at 653, 631, and 624 cm^{-1}.

Assignment of sulfate ion absorption bands in the IR and Raman spectra of compound III was performed using data from ref. [6]. In the IR spectrum, the symmetric stretching mode ν_1 appears at 986 cm^{-1}; (ν_1=971 cm^{-1} in Raman spectrum), and the asymmetric stretching ν_3 appears at 1120 cm^{-1} (Raman spectrum: 1111 cm^{-1}). The bending mode ν_4 is observed as a doublet at 681 and 610 cm^{-1} in IR (Raman spectrum: 682, 648, and 623 cm^{-1}), while ν_2 appears as a doublet at 436 and 433 cm^{-1} (Raman: 477 and 434 cm^{-1}).

In the IR spectrum of compound **II**, the asymmetric stretching vibrations $\nu_{as}(SO_2)$ appear as a strong-intensity doublet at 1234 and 1208 cm^{-1}. The symmetric stretching $\nu_s(SO_2)$ is represented by a multiplet of lines with varying intensity in the 1180–1030 cm^{-1} region. The S–O stretching vibration is seen as a high-intensity doublet at 551 and 547 cm^{-1}. The zwitterionic structure of compound **II** is supported by the observation that the position of the ν(NH) band in the IR spectrum shows no significant shift, similar to aminomethanesulfonic acid (AMSA) and its N-alkylated derivatives [6].

Upon attempted recrystallization from aqueous solution, the ammonium sulfite salt MiPA (**I**) undergoes hydrolytic sulfoxidation, converting into the corresponding sulfate **III**. Similarly, the N-alkylated AMSA derivative **II** is oxidized via a hydrolytic redox process to sulfate III as well.

Thus, chemisorption of SO_2 in aqueous MiPA solution leads to the formation of ammonium sulfite (reaction (1)). Upon addition of formaldehyde, a condensation reaction occurs (reaction (2)), accompanied by sulfoxidation of S(IV) to S(VI), yielding an N-alkylated AMSA derivative of zwitterionic structure (similar to [6]). However, these compounds are unstable in aqueous solution in the presence of atmospheric oxygen (reactions (3) and (4)).

Table 2

Bond lengths in the structure of compound III

Bond	Bond length, Å	Bond	Bond length, Å	Bond	Bond length, Å
S(1)–O(4)	1.468(2)	O(9)–C(2)	1.376(6)	O(11)–C(8)	1.415(5)
S(1)–O(3)	1.468(2)	N(1)–C(1)	1.464(5)	N(3)–C(7)	1.468(4)
S(1)–O(2)	1.470(2)	C(1)–C(2)	1.418(6)	C(7)–C(8)	1.525(5)
S(1)–O(1)	1.475(2)	C(2)–C(3)	1.548(6)	C(8)–C(9)	1.503(5)
S(2)–O(7)	1.457(2)	O(10)–C(5)	1.411(5)	O(12)–C(11)	1.359(5)
S(2)–O(5)	1.464(2)	N(2)–C(4)	1.462(4)	N(4)–C(10)	1.467(4)
S(2)–O(6)	1.467(2)	C(4)–C(5)	1.508(5)	C(10)–C(11)	1.432(5)
S(2)–O(8)	1.467(2)	C(5)–C(6)	1.515(5)	C(11)–C(12)	1.520(6)

Table 3

Bond valence angles in the structure of compound III

Bond	Bond angle, ^{0}	Bond	Bond angle, ^{0}
O(4)–S(1)–O(3)	111.40(14)	O(9)–C(2)–C(3)	108.4(4)
O(4)–S(1)–O(2)	109.60(13)	C(1)–C(2)–C(3)	111.3(4)
O(3)–S(1)–O(2)	108.63(13)	N(2)–C(4)–C(5)	111.6(3)
O(4)–S(1)–O(1)	109.34(14)	O(10)–C(5)–C(4)	111.6(3)
O(3)–S(1)–O(1)	109.14(13)	O(10)–C(5)–C(6)	108.4(4)
O(2)–S(1)–O(1)	108.68(14)	C(4)–C(5)–C(6)	111.2(3)
O(7)–S(2)–O(5)	109.38(14)	N(3)–C(7)–C(8)	110.2(3)
O(7)–S(2)–O(6)	109.51(13)	O(11)–C(8)–C(9)	108.1(4)
O(5)–S(2)–O(6)	108.85(14)	O(11)–C(8)–C(7)	111.2(3)
O(7)–S(2)–O(8)	111.19(15)	C(9)–C(8)–C(7)	110.5(3)
O(5)–S(2)–O(8)	109.30(13)	C(11)–C(10)–N(4)	115.3(3)
O(6)–S(2)–O(8)	108.57(13)	O(12)–C(11)–C(10)	119.2(4)
C(2)–C(1)–N(1)	116.6(4)	O(12)–C(11)–C(12)	106.1(4)
O(9)–C(2)–C(1)	117.3(5)	C(10)–C(11)–C(12)	112.5(4)

$$2CH_3CH(OH)CH_2NH_2+SO_2+H_2O\rightarrow \rightarrow[CH_3CH(OH)CH_2NH_3]_2SO_3 \quad (1)$$

$$CH_3CH(OH)CH_2NH_2+SO_2+CH_2O+H_2O\rightarrow \rightarrow CH_3CH(OH)CH_2N^+H_2CH_2SO_3^- \quad (2)$$

$$[[CH_3CH(OH)CH_2NH_3]_2SO_3+ +1/2O_2 \xrightarrow{H_2O} [CH_3CH(OH)CH_2NH_3]_2SO_4 \quad (3)$$

$$2CH_3CH(OH)CH_2N^+H_2CH_2SO_3^-+2H_2O\rightarrow \rightarrow[CH_3CH(OH)CH_2NH_3]_2SO_4+SO_2\uparrow+ +CH_2O\uparrow+CH_3OH\uparrow \quad (4)$$

This is the second known case where the product of the interaction between an ethanolamine derivative and SO_2 (the corresponding ammonium sulfite) undergoes hydrolytic sulfooxidation of S(IV) to S(VI) in the presence of atmospheric oxygen, forming ammonium sulfate (reaction (3)), similarly to [6,14]. In the case of tris(hydroxymethyl)methylamine (TRIS), from the reaction medium

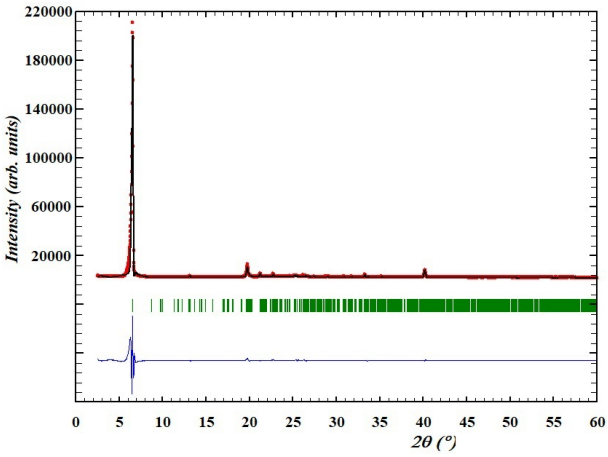

Fig. 3. Rietveld refinement for powder diffractogram of compound **III**. Experimental pattern is shown as red circles; calculated pattern is shown as black line; vertical bars show the Bragg position for lines; bottom line shows the difference between experimental and calculated intensities in every point

Table 4

Hydrogen bonds D–H···A in the structure of compound III

D–H···A	d(D–H), Å	d(H···A), Å	d(D···A), Å	∠(DHA), ^{0}
N(1)–H(1A)···O(6)^1	0.89	2.07	2.924(3)	160.7
N(1)–H(1A)···O(8)^1	0.89	2.55	3.139(4)	124.3
N(1)–H(1B)···O(1)^2	0.89	2.21	2.991(3)	146.5
N(1)–H(1B)···O(1)^1	0.89	2.38	2.981(4)	125.2
N(1)–H(1C)···O(2)^1	0.89	2.52	2.954(4)	110.6
N(1)–H(1C)···O(7)	0.89	2.20	2.985(4)	146.6
O(9)–H(9)···O(7)	0.82	1.97	2.788(4)	179.2
O(10)–H(10)···O(5)	0.82	1.98	2.770(3)	162.7
N(2)–H(2A)···O(3)^3	0.89	1.99	2.860(4)	166.3
N(2)–H(2B)···O(2)^4	0.89	1.93	2.799(3)	163.4
N(2)–H(2C)···O(5)	0.89	2.64	3.147(3)	117.4
N(2)–H(2C)···O(8)	0.89	1.97	2.864(3)	176.7
C(4)–H(4D)···O(11)	0.97	2.62	3.315(5)	128.4
O(11)–H(11)···O(1)	0.82	1.94	2.749(3)	166.8
N(3)–H(3A)···O(1)	0.89	2.63	3.166(3)	119.4
N(3)–H(3A)···O(3)	0.89	1.98	2.867(3)	179.8
N(3)–H(3B)···O(6)^1	0.89	1.94	2.800(3)	161.5
N(3)–H(3C)···O(8)	0.89	1.97	2.845(4)	168.9
O(12)–H(12)···O(4)	0.82	1.97	2.769(4)	165.5
N(4)–H(4A)···O(4)	0.89	2.24	3.005(3)	144.6
N(4)–H(4A)···O(6)^4	0.89	2.47	2.926(4)	112.4
N(4)–H(4B)···O(5)^6	0.89	2.18	2.972(3)	147.4
N(4)–H(4B)···O(5)^4	0.89	2.43	3.017(4)	123.6
N(4)–H(4C)···O(2)^7	0.89	2.07	2.922(3)	160.3
N(4)–H(4C)···O(3)^7	0.89	2.54	3.144(4)	126.1

Notes: Symmetry transformations for atom A: ^{1} – −x+1,−y+1,−z+1; ^{2} – x,y+1,z; ^{3} – x−1,y,z; ^{4} – −x+1,−y,−z+1; ^{5} – x+1,y,z; ^{6} – x+1,y−1,z; ^{7} – −x+2,−y,−z+1.

SO_2–TRIS–CH_2O–H_2O, a product of incomplete hydrolytic decomposition of the corresponding N-alkylated AMSA derivative, $[(HOCH_2)_3CN^+H_3][HOCH_2SO_3^-]$, was isolated [6]. The compound $CH_3CH(OH)CH_2N^+H_2CH_2SO_3^-$, in contrast, undergoes more complete hydrolysis to ammonium sulfate, $[CH_3CH(OH)CH_2NH_3]_2SO_4$, (reaction (4)).

REFERENCES

1. *Kondratenko Y.A.* From alkanolamines to protic alkanolammonium ionic liquids // J. Mol. Liq. – 2024. – Vol.409. – Art. No. 125460.

2. *Luis P.* Use of monoethanolamine (MEA) for CO_2 capture in a global scenario: consequences and alternatives // Desalination. – 2016. – Vol.380. – P.93-99.

3. *Carbon* dioxide capture using liquid absorption methods: a review / Ochedi F.O., Yu J., Yu H., Liu Y., Hussain A. // Environ. Chem. Lett. – 2021. – Vol.19. – P.77-109.

4. *Mono-* and bifunctional impregnated fiber chemosorbents for respiratory purpose / Ennan A.A.-A., Khoma R.E., Dlubovskii R.M., Zukharenko Yu.S., Benkovska T.S., Knysh I.M. // Visn. Odes. Nac. Univ. Him. – 2022. – Vol.27. – No. 1. – P.6-36.

5. *Polymorphism* with conformational isomerism and incomplete crystallization in solid ethanolamine / Romanini M., Negrier P., Tripathi P., Lira K.M., Gournis D., Barrio M., et al. // Cryst. Growth Des. – 2019. – Vol.19. – No. 11. – P.6360-6369.

6. *Khoma R.E.* Acid-base interaction and sulfooxidation at chemosorption of sulfur dioxide by alkylamines aqueous solutions: Thesis of Doctor's degree dissertation: 02.00.01. – Kyiv, 2019. – 427 p.

7. *Products* of interaction between sulfur(IV) oxide and aqueous solutions of hexamethylendiamine and tert-butylamine: the crystal structure of hexamethylenediammonium sulfate dihydrate / Khoma R.E., Ennan A.A., Shishkin O.V., Baumer V.N., Gelmboldt V.O. // Russ. J. Inorg. Chem. – 2012. – Vol.57. – No. 12. – P.1559-1562.

8. *Sheldrick G.M.* SHELXT – Integrated space-group and crystal-structure determination // Acta Cryst. A. – 2015. – Vol.71. – P.3-8.

9. *Sheldrick G.M.* Crystal structure refinement with SHELXL // Acta Cryst. C. – 2015. – Vol.71. – P.3-8.

10. *Farrugia L.J.* WinGX and ORTEP for Windows: an update // J. Appl. Cryst. – 2012. – Vol.45. – P.849-854.

11. *Cacela C., Fausto R., Duarte M.L.* A combined matrix-isolation infrared spectroscopy and MO study of 1-amino-2-propanol // Vib. Spectrosc. – 2001. – Vol.26. – No. 1. – P.113-131.

12. *Vul'fson N.S., Zaikin V.G., Mikaya A.I.* Mass spectrometry of organic compounds. – M.: Khimiya, 1986. – 312 p.

13. *Tam C.N., Bour P., Keiderling T.A.* An experimental comparison of vibrational circular dichroism and Raman optical activity with 1-amino-2-propanol and 2-amino-1-propanol as model compounds // J. Am. Chem. Soc. – 1997. – Vol.119. – No. 30. – P.7061-7064.

14. *Synthesis* and spectral characteristics of tris(hydroxymethyl)methylammonium sulfite / Khoma R.E., Gelmboldt V.O., Ennan A.A., Baumer V.M., Dlubovskii R.M., Vodzinskii S.V. // Voprosy Khimii i Khimicheskoi Tekhnologii. – 2020. – No. 4. – P.172-176.

Received 26.09.2025

СПЕКТРАЛЬНІ ХАРАКТЕРИСТИКИ ПРОДУКТІВ ВЗАЄМОДІЇ В СИСТЕМАХ SO_2–$CH_3CH(OH)CH_2NH_2$–H_2O ТА SO_2–$CH_3CH(OH)CH_2NH_2$–CH_2O–H_2O

Р.Є. Хома, В.М. Баумер, В.О. Гельмбольдт, Н.Ф. Федько, В.В. Менчук, С.В. Водзінський, Ю.В. Ішков, І.М. Ракіпов, Д.В. Менчук

При взаємодії в системах «діоксид сірки–2-гідро- ксипропіламін (МіРА)–вода» та «діоксид сірки–МіРА–параформ–вода» утворюються сульфіт 2-гідроксипропіламонію $[CH_3CH(OH)CH_2NH_3]_2SO_3$ (**I**) та N-(2-гідрокси-пропіл)амінометансульфокислота $CH_3CH(OH)CH_2N^+H_2CH_2SO_3^-$ (**II**), відповідно. Вказані сполуки при незалежній перекристалізації із водного розчину в результаті гідролітичних перетворень перетворюються в сульфат 2-гідроксипропіламонію $[CH_3CH(OH)CH_2NH_3]_2SO_4$ (**III**). Одержані продукти охарактеризовано методами елементного та рентгеноструктурного аналізу, ІЧ-, КР, ЯМР ^1H та ^{13}C спектроскопії, а також мас-спектрометрії. Сполука **III** кристалізується в триклінній сингонії (просторова група P-1, a=9,0753(8), b=10,3038(7), c=13,6845(14) Å , α=99,491(7), β=94,712(8), γ=90,119(7)^0, V=1257.7(2) Å^3, Z=4). ІЧ-спектр солі **I** показує валентні коливання сульфіт-аніона ν(SO) (ν_1 та ν_3), представлені смугами при 912 та 954 см$^{-1}$, відповідно. Коливання іона δ_s (ν_2) спостерігається в ІЧ-спектрі у вигляді відносно інтенсивних смуг при 610 та 621 см$^{-1}$. В ІЧ-спектрі сполуки II коливання $\nu_{as}(SO_2)$ проявляються дублетом при 1234 та 1208 см$^{-1}$; $\nu_s(SO_2)$ надано мультиплетом ліній на ділянці 1180–1030 см$^{-1}$. При спробі перекристалізації з водного розчину сульфіт амонію МіРА (**I**) піддається гідролітичному сульфоокисленню, перетворюючись на відповідний сульфат **III**. Аналогічно, N-алкілована похідна AMSA II також окислюється гідролітичним окисно-відновним процесом до сульфату III.

Ключові слова: діоксид сірки; 2-гідроксипропіламін; амонієвий сульфіт; амонієвий сульфат; конденсація; сульфоокиснення; спектральні характеристики.

SPECTRAL CHARACTERISTICS OF INTERACTION PRODUCTS IN SO_2–$CH_3CH(OH)CH_2NH_2$–H_2O AND SO_2–$CH_3CH(OH)CH_2NH_2$–CH_2O–H_2O SYSTEMS

R.E. Khoma [a, *], V.N. Baumer [b], V.O. Gelmboldt [c], N.F. Fedko [a], V.V. Menchuk [a], S.V. Vodzinsky [a], Yu.V. Ishkov [a], I.M. Rakipov [d], D.V. Menchuk [a]

[a] Odesa I.I. Mechnikov National University, Odesa, Ukraine

[b] Institute for Single Crystals, National Academy of Sciences of Ukraine, Kharkiv, Ukraine

[c] Odesa National Medical University, Odesa, Ukraine

[d] A.V. Bogatsky Physico-Chemical Institute, National Academy of Sciences of Ukraine, Odesa, Ukraine

[*] e-mail: rek@onu.edu.ua

Interaction in the systems «sulfur(IV) oxide–2-hydroxypropylamine (MiPA)–water» and «sulfur(IV) oxide–MiPA–paraform–water» leads to the formation of 2-hydroxypropylammonium sulfite $[CH_3CH(OH)CH_2NH_3]_2SO_3$ (I) and N-(2-hydroxypropyl)aminomethanesulfonic acid $CH_3CH(OH)CH_2N^+H_2CH_2SO_3^-$ (II), respectively. These compounds, upon independent recrystallization from aqueous solution, are transformed into 2-hydroxypropylammonium sulfate $[CH_3CH(OH)CH_2NH_3]_2SO_4$ (III) as a result of hydrolytic transformations. The obtained products were characterized by the methods of elemental and X-ray structural analysis, IR, Raman, ^1H and ^{13}C NMR spectroscopy, and mass spectrometry. Compound III crystallizes in triclinic class (space group P-1, a=9.0753(8) Å, b=10.3038(7) Å, c=13.6845(14) Å, α=99.491(7)^0, β=94.712(8)^0, γ=90.119(7)^0, V=1257.7(2) Å^3, Z=4). The IR spectrum of salt I shows the valence vibrations of ν(SO) sulfite anion (ν_1 and ν_3), represented by bands at 912 and 954 cm^{-1}, respectively. The vibration δ_s (ν_2) of SO_3^{2-} ion is observed in the IR spectrum as relatively intense bands at 610 and 621 cm^{-1}. In the IR spectrum of compound II, the vibrations $\nu_{as}(SO_2)$ appear as a doublet at 1234 and 1208 cm^{-1}; $\nu_s(SO_2)$ is represented by a multiplet of lines in the 1180–1030 cm^{-1} region. Upon attempted recrystallization from aqueous solution, the ammonium sulfite salt MiPA (I) undergoes hydrolytic sulfoxidation, converting into the corresponding sulfate III. Similarly, the N-alkylated AMSA derivative II is oxidized via a hydrolytic redox process to sulfate III as well.

Keywords: sulfur dioxide; 2-hydroxypropylamine; ammonium sulfite; ammonium sulfate; condensation; sulfoxidation; spectral characteristics.

REFERENCES

1. Kondratenko YA. From alkanolamines to protic alkanolammonium ionic liquids. *J Mol Liq*. 2024; 409: 125460. doi: 10.1016/j.molliq.2024.125460.

2. Luis P. Use of monoethanolamine (MEA) for CO_2 capture in a global scenario: consequences and alternatives. *Desalination*. 2016; 380: 93-99. doi: 10.1016/j.desal.2015.08.004.

3. Ochedi FO, Yu J, Yu H, Liu Y, Hussain A. Carbon dioxide capture using liquid absorption methods: a review. *Environ Chem Lett*. 2021; 19: 77-109. doi: 10.1007/s10311-020-01093-8.

4. Ennan AA, Khoma RE, Dlubovskii RM, Zukharenko YuS, Benkovska TS, Knysh IM. Mono- and bifunctional impregnated fiber chemosorbents for respiratory purpose. *Odesa National University Herald Chemistry*. 2022; 27(1): 6-36. (*in Ukrainian*). doi: 10.18524/2304-0947.2021.4(80).248297.

5. Romanini M, Negrier P, Tripathi P, Lira KM, Gournis D, Barrio M, et al. Polymorphism with conformational isomerism and incomplete crystallization in solid ethanolamine. *Cryst Growth Des*. 2019; 19(11): 6360-6369. doi: 10.1021/acs.cgd.9b00836.

6. Khoma RE. *Kyslotno-osnovna vzaiemodiia ta sulfookysnennia pry khemosorbtsii oksydu sulfuru (IV) vodnymy rozchynamy alkilaminiv* [Acid-base interaction and sulfooxidation at chemosorption of sulfur(IV) dioxide by alkylamines aqueous solutions] [dissertation]. Kyiv (Ukraine): V.I. Vernadsky Institute of General and Inorganic Chemistry of the NAS of Ukraine; 2019. 427 p. (*in Ukrainian*).

7. Khoma RE, Ennan AA, Shishkin OV, Baumer VN, Gelmboldt VO. Products of interaction between sulfur(IV) oxide and aqueous solutions of hexamethylendiamine and tert-butylamine: the crystal structure of hexamethylenediammonium sulfate dihydrate. *Russ J Inorg Chem*. 2012; 57(12): 1559-1562. doi: 10.1134/S003602361212008X.

8. Sheldrick GM. SHELXT – Integrated space-group and crystal-structure determination. *Acta Cryst A*. 2015; 71: 3-8. doi: 10.1107/s2053273314026370.

9. Sheldrick GM. Crystal structure refinement with SHELXL. *Acta Cryst C*. 2015; 71: 3-8. doi: 10.1107/S2053229614024218.

10. Farrugia LJ. WinGX and ORTEP for Windows: an update. *J Appl Cryst*. 2012; 45: 849-854. doi: 10.1107/S0021889812029111.

11. Cacela C, Fausto R, Duarte ML. A combined matrix-isolation infrared spectroscopy and MO study of 1-amino-2-propanol. *Vib Spectrosc*. 2001; 26(1): 113-131. doi: 10.1016/S0924-2031(01)00112-6.

12. Vul'fson NS, Zaikin VG, Mikaya AI. *Mass spectrometry of organic compounds*. Moscow: Khimiya; 1986. 312 p. (*in Russian*).

13. Tam CN, Bour P, Keiderling TA. An experimental comparison of vibrational circular dichroism and Raman optical activity with 1-amino-2-propanol and 2-amino-1-propanol as model compounds. *J Am Chem Soc*. 1997; 119(30): 7061-7064. doi: 10.1021/ja963239h.

14. Khoma RE, Gelmboldt VO, Ennan AA, Baumer VM, Dlubovskii RM, Vodzinskii SV. Synthesis and spectral characteristics of tris(hydroxymethyl)methylammonium sulfite. *Voprosy Khimii i Khimicheskoi Tekhnologii*. 2020; (4): 172-176. (*in Ukrainian*). doi: 10.32434/0321-4095-2020-131-4-172-176.